Journal of Magnetism and Magnetic Materials 519 (2021) 167441

Contents lists available at ScienceDirect

Journal of Magnetism and Magnetic Materials

journal homepage: www.elsevier.com/locate/jmmm

Research articles

Particle size-dependent magnetic hyperthermia in gadolinium silicide micro- and nano-particles from calorimetry and AC magnetometry

Z. Boekelheide [a,*], S. Hunagund [b], Z.A. Hussein [a], Jackson T. Miller [a], A.A. El-Gendy [c], R. L. Hadimani [b,d,*]

[a] Department of Physics, Lafayette College, Easton, PA 18042, USA
[b] Department of Mechanical and Nuclear Engineering, Virginia Commonwealth University, Richmond, VA 23284, USA
[c] Department of Physics, University of Texas at El Paso, El Paso, TX 79968, USA
[d] Department of Biomedical Engineering, Virginia Commonwealth University, Richmond, VA 23284, USA

A R T I C L E I N F O

Keywords:
Biomagnetics
Silicides
Hyperthermia

A B S T R A C T

Self-regulating magnetic hyperthermia, in which heating of magnetic particles is limited by the magnetic transition temperature, could be a valuable form of magnetic hyperthermia for cancer treatment, as it can ensure uniform heating across tumor tissue. Gadolinium silicide has been suggested as a candidate material for self-regulating magnetic hyperthermia because of its high magnetization, Curie temperature near the desired treatment temperature, and tunability. Previous measurements of polydisperse micro- and nano-particles prepared from ball-milled Gd_5Si_4 yielded a decreased Curie temperature T_C with a broad transition, suggesting that particle size may be used to tune T_C. Other studies of size-selected particles of ball-milled Gd_5Si_4 showed decreased T_C and magnetization with decreased particle size, but increased coercivity with decreased size, and the combined effects on the specific loss power were unknown. This work presents measurements of the particle size-dependence of the specific loss power of ball-milled Gd_5Si_4, showing that the largest particles (approx. 780 nm) behave similarly to the previously measured polydisperse samples, while the smaller particles all have decreased specific loss power. Dynamic hysteresis loop measurements show that the coercivity of the particles is increased under the conditions used for magnetic hyperthermia (particles dispersed in water, under an alternating magnetic field) relative to quasistatic measurements of powder samples, though a particle size-dependence of the coercivity was not observed under hyperthermia conditions. This work highlights one of the challenges of implementing self-regulating magnetic hyperthermia: in general, materials tend to have low coercivity near the magnetic transition temperature. Given this challenge, rare-earth compounds with high magnetization may provide the best opportunity to obtain significant heating for self-regulating hyperthermia.

1. Introduction

Magnetic hyperthermia is a potential cancer treatment currently undergoing much research and development[1,2]. In magnetic hyperthermia for cancer treatment, magnetic particles are directed toward a cancerous tumor and an alternating magnetic field (AMF) is applied, causing rapid switching of the particles' magnetic moments resulting in dissipated heat equal to the area enclosed in the magnetic hysteresis loop $M(H)$ during each field cycle. Temperatures in the optimal range of 43–45 °C can damage or kill cells of the tumor without damage to normal cells[3]. Such temperatures can also prevent cancer cells from repairing damaged DNA, so hyperthermia can be used as an adjuvant to enhance other therapies such as radiation which work by damaging tumor DNA to control cell growth[4,5]. The magnitude of heat produced by a given material is described by the specific loss power (SLP), or the power dissipated per gram of material.

Self-regulating magnetic hyperthermia is a variation of magnetic hyperthermia in which the magnetic particles used have a magnetic transition temperature T_C around the desired treatment temperature so that magnetic heating only occurs up to that limiting temperature[3]. This can prevent overheating and subsequent damage to healthy cells. It can also help maintain a uniform temperature within the whole tumor volume and at the margins, which otherwise must be achieved by carefully controlling particle distribution and magnetic field strength in

* Corresponding authors.
E-mail addresses: boekelhz@lafayette.edu (Z. Boekelheide), rhadimani@vcu.edu (R.L. Hadimani).

https://doi.org/10.1016/j.jmmm.2020.167441
Received 16 April 2020; Received in revised form 22 September 2020; Accepted 23 September 2020
Available online 8 October 2020

the cancerous region, a technical challenge[6,7].

Several candidate materials have been proposed for self-regulated hyperthermia, typically compounds or alloys in which the stoichiometry can be varied to tune the Curie temperature [3,8]. One candidate material for self-regulated hyperthermia is Gd_5Si_4 and related alloys [9–11]. Bulk Gd_5Si_4 has a high magnetization with $T_C = 63\ ^\circ C$, only 20 °C above the desired treatment temperature for hyperthermia [12]. Our previous work has shown that ball-milling of Gd_5Si_4 to form micro- and nano-particles results in a decreased T_C, which is promising for potential tunability[13,10,14,15]. Ball-milling results in highly polydisperse samples; previously we showed that micro- and nano-particles from ball-milled Gd_5Si_4 with individual particles ranging from tens of nm to several μm had a T_C of 50 °C; however, the transition was broad (28 °C) [10].

The change in T_C with ball-milling and the broad transition in a polydisperse sample suggests that microstructural factors control the magnetic properties. Recent studies of the size-dependence of magnetic and structural properties of ball-milled gadolinium silicide samples showed that T_C and magnetization decreased with decreasing particle size[16]. In addition, coercivity increased with decreasing particle size [16], consistent with expectations[17,18]. Thus, we sought to investigate the size dependence of the SLP. In addition to desiring high SLP and T_C in the therapeutic range, particles below a few hundred nm in size are preferable for magnetic hyperthermia because they accumulate preferentially in tumors[19,20]. Thus, in this paper, we probe whether smaller particles, which are more appropriate for hyperthermia, have promising magnetothermal properties. We also use dynamic hysteresis loops to probe the coercivity of these particles under conditions of hyperthermia (dispersed in H_2O, under an alternating magnetic field rather than a quasistatic field).

2. Experimental methods

Initially, a sample of polydisperse gadolinium silicide particles was prepared by grinding arc-melted Gd_5Si_4 into a powder and then ball-milling, the details of which have been described previously[10]. For size-separation, the particles were suspended in ethanol and ferromagnetic particles were extracted from the mixture using a grade N52 NdFeB permanent magnet. Then, the ferromagnetic particles were suspended in ethanol and samples were collected from the sediment obtained after the following times: 50 min, 3 h 30 min, 17 h, 96 h. The supernatant left after 96 h formed an additional sample. The samples are named S1, S2, S3, S4, and S5, respectively (see Table 1).

Previous work has characterized the crystal phases of both polydisperse and size-selected gadolinium silicide powders prepared in this manner. XRD analysis on the ball-milled gadolinium silicide powder before any size-separation procedure has shown the presence of Gd_5Si_4 as the major phase and GdSi, Gd_5Si_3 as the minor phases in the sample [10]. Previous studies of size-separated gadolinium silicide powders suggest that the fraction of Gd_5Si_3 may be higher in the smaller particles [16].

The particle size, morphology, and DC magnetic properties of the size-separated gadolinium silicide particles were characterized using scanning electron microscopy (SEM, Hitachi Model SU-70) and a vibrating sample magnetometer (VSM, Quantum Design, 3T Versalab). The average particle size distribution in each sample was determined by individually measuring the diameters of the particles using image analysis software (ImageJ) from the SEM digital images.

For the SLP measurements, the ethanol in which the particles were suspended was replaced with water. Using a rare earth magnet to localize the particles, the ethanol was removed and replaced with deionized water, with three rinse steps. Then, a small amount of polyethylene glycol (PEG) was added to stabilize the particles. The magnetic hyperthermia measurements were performed on each sample of particles dispersed in 500 μL of H_2O with 6 mg/mL of PEG in a flat-bottomed glass vial. The particle concentration was approximately 20 mg/mL for S1-4, while the concentration of S5 was significantly lower, at 1 mg/mL, because of the small amount of sample left in the supernatant.

To measure the SLP calorimetrically, an Ambrell EasyHeat AMF generator with an eight-turn, water-cooled solenoidal coil was used, operating at a frequency of 224^{+2}_{-4} kHz. The field strength in the center of the coil was calibrated using a Fluxtrol alternating magnetic field probe. The applied field strength $\mu_0 H_{max}$ is given in terms of the root mean square (rms) field strength: $\mu_0 H_{max} = \sqrt{2}\mu_0 H_{rms}$ because the field amplitude is not exactly the same for each cycle.

The sample was placed at the center of the solenoid and the AMF was applied while the temperature of the sample as a function of time ($T(t)$) was monitored using a fiber-optic sensor (Opsens OTG-M170). The sample starting temperature was 21.0 °C, and the current was applied until the temperature reached at least 22.0 °C, at which point the AMF was removed and the sample was allowed to cool to 21.0 °C. The process was repeated for a range of AMF amplitudes from 0–0.064 T. The SLP was calculated from the initial slope of the temperature rise upon application of the AMF, where “initial” refers to the first degree of temperature rise ignoring 0.1 ° at each endpoint (e.g. 21.1–21.9 °C). $T(t)$ was linear in this temperature range for all runs for which the SLP was calculated, according to the equation:

$$\mathrm{SLP} = \frac{c m_w}{m_p}\left(\frac{dT}{dt}\right)_{\mathrm{initial}}. \tag{1}$$

Here, c is the specific heat capacity of water, m_w is the mass of water, and m_p is the mass of the particles. The heat capacity of the sample is assumed to be dominated by the water. The same procedure was performed on a water blank to determine background heating, and this background heating slope was subtracted from the sample heating slopes to find the heating specific to the magnetic samples. The losses in this temperature range, which were small, were also subtracted to obtain a corrected slope[21]. The variation between multiple trials leads to an uncertainty in the SLP measurement of 15%, presumably due to slight sedimentation. A larger uncertainty was observed in sample S5 because of the low concentration leading to a small slope dT/dt.

Dynamic hysteresis loop measurements, a form of AC magnetometry, were performed on samples S1 and S3, dispersed in H_2O with a concentration of 80 mg/mL, and on a polydisperse powder sample. The dynamic hysteresis loop measurements utilize the same solenoidal coil and AMF generator as the SLP measurements; within the coil, a pickup coil assembly made from 36 gauge phosphor bronze wire wound around a 1/2 inch hollow polycarbonate form is placed. The pickup coil assembly consists of two counterwound 3-turn coils in series, such that, in the absence of a sample, the inductive signal from each coil cancels and the emf across the coil assembly is zero, similar to that utilized by Garaio et al.[22]. When a sample in a 0.3 mL vial (PELCO) is inserted into one of the coils, then any signal is due only to the magnetization (M) of the sample. Before a measurement, the empty pickup coil assembly is centered within the solenoidal coil by translating it along the axis of the solenoid until the signal is minimized; an empty measurement is taken at this point which will be subtracted from the sample signal.

The emf across the pickup coil assembly is measured by an oscillo-

Table 1
Physical and magnetic properties of the size-selected samples.

Sample	Sedimentationtime	Avg. particlesize (nm)	M_{sat}(emu/g)at 300 K	T_C(K)	SLP(W/g) at 0.064 T
S1	50 min	780	62	315^{+19}_{-13}	24 ± 4
S2	3 h 30 min	610	31	311^{+17}_{-19}	4.4 ± 0.7
S3	17 h	560	20	305^{+15}_{-67}	5.6 ± 1.0
S4	96 h	300	18	261^{+44}_{-38}	2.6 ± 0.4
S5	supernatant	140	3.8	244^{+28}_{-101}	2 ± 5

scope (Tektronix MDO3024). The applied field (H) is measured by a separate pickup coil external to the application coil. The oscilloscope measures the emfs across both pickup coils, which are proportional to dM/dt and dH/dt. The empty signal is subtracted from the sample signal, and then these signals are corrected for the frequency-dependent impedance of the pickup coil assembly including 48 inch BNC transmission cables (characterized by a Rohde & Schwartz ZND vector network analyzer)[22]. The frequency-corrected signals are integrated to obtain $M(t)$ and $H(t)$ and then a plot of $M(H)$ is produced. The temperature of the sample is monitored during the dynamic hysteresis loop measurements using an Opsens fiber-optic temperature sensor; hysteresis loops can be obtained at a variety of temperatures either utilizing the samples' intrinsic heating or by heating/cooling the sample externally.

3. Results

Fig. 1 shows SEM images of the size-selected particles, showing that longer sedimentation times lead to smaller average size, as expected. The average particle sizes ranged from 780 nm (S1 - 50 min) to 140 nm (S5 - supernatant).

The magnetization M as a function of temperature T, measured in an applied field of 0.02 T, (Fig. 2(a)) shows that the Curie transition temperature decreases with decreasing particle size. There is also a general trend of decreasing magnetization with decreasing particle size, although the trend is only monotonic at temperatures above 265 K. Below 265 K, the magnetization of sample S4 exceeds that of S3 and, at some temperatures, S2. The temperature derivative of magnetization, dM/dT is shown in Fig. 2(b). These data show an inverse peak in dM/dT for each sample, with the peak occurring at lower temperatures for the smaller particle samples. The peak in dM/dT also broadens significantly as particle size decreases. The Curie temperature for each sample, found from the peak in the dM/dT vs. T curve, is tabulated in Table 1. The (asymmetric) width of the transition is described by the position of the half-maximum value on the positive and negative side of the peak in dM/dT. The decrease in Curie temperature with particle size is likely due to the disorder/defects and/or microstrains introduced during the ball-milling process, which differ for particles of different sizes.

$M(H)$ at 300 K is shown in Fig. 3. Again, the trend of decreasing magnetization with decreasing particle size is visible. Ferromagnetic (nonlinear) behavior is observed in all samples. A linear background is also observed, which may be due to a fraction of paramagnetic Gd_5Si_3. The saturation magnetization, determined from the magnetization at 300 K and 3 T, is shown in Table 1.

The SLP is shown in Fig. 4(a) and compared to data from a polydisperse gadolinium silicide sample[10]. The magnitude of the SLP for the sample of the largest particles, S1, is similar to the magnitude of the SLP for polydisperse Gd_5Si_4 samples at high fields, but smaller at low fields. The magnitude of the SLP is lower for all of the samples of smaller particles. To compare the magnitudes more directly, the SLPs at the highest field, 0.064 T, are shown in Fig. 4(b) for the size-selected samples and the previously measured polydisperse sample from [10]. The

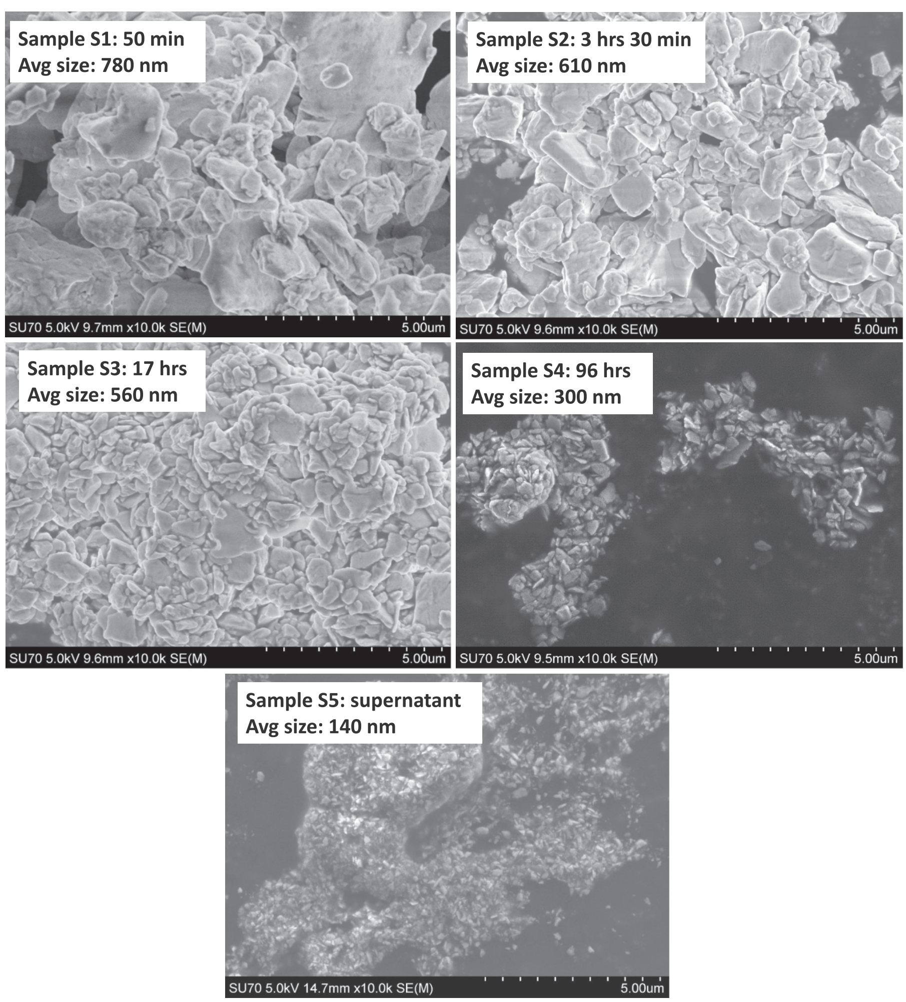

Fig. 1. Scanning Electron Microscopy (SEM) images of size-selected gadolinium silicide particles showing the decrease in average particle size with sedimentation time.

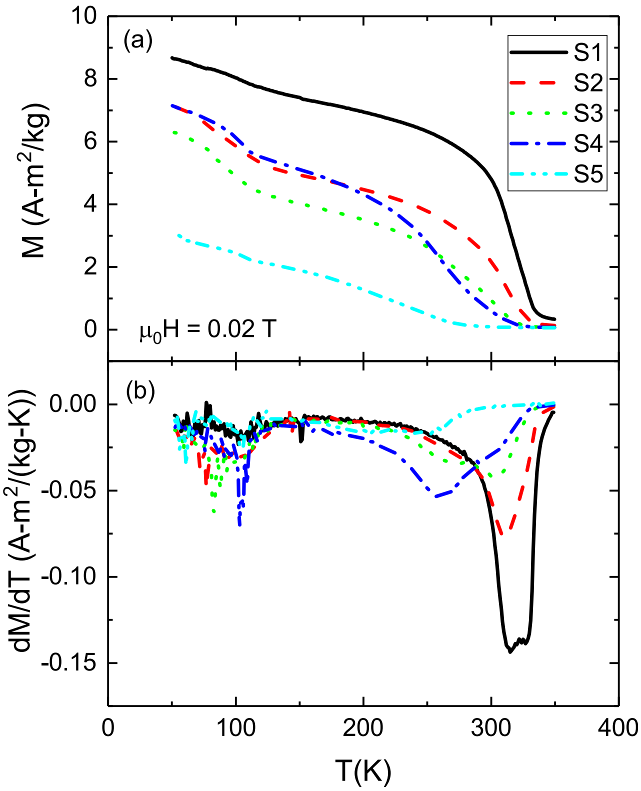

Fig. 2. (a) Magnetization (M) as a function of temperature (T) at a magnetic field of 0.02 T for the five powder samples, measured by VSM. (b) dM/dT as a function of temperature (T) extracted from the data in (a).

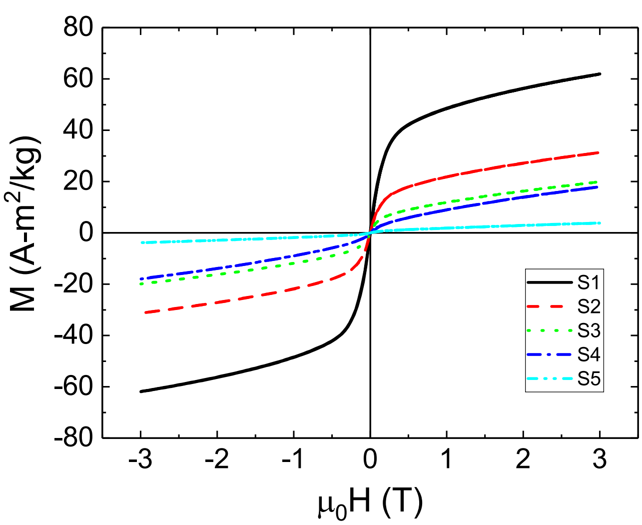

Fig. 3. Magnetic hysteresis loops at 300 K for the five powder samples, measured by VSM.

sample with the largest particle size has similar SLP to the polydisperse sample while the samples with smaller particle size have lower SLP. This suggests that the heating observed in the polydisperse sample was dominated by the larger particles.

To further understand the magnetic properties underpinning the SLP results, we undertook dynamic hysteresis loop measurements of samples S1 and S3 dispersed in H_2O, and of a polydisperse powder sample, at a range of temperatures. These are shown in Fig. 5. The data show that the hysteresis loops are narrow with low coercivity; the coercivity and the area enclosed in the loops (which is proportional to energy loss) decreases significantly with increasing temperature as the materials approach their respective T_C. Paramagnetic behavior is seen above T_C.

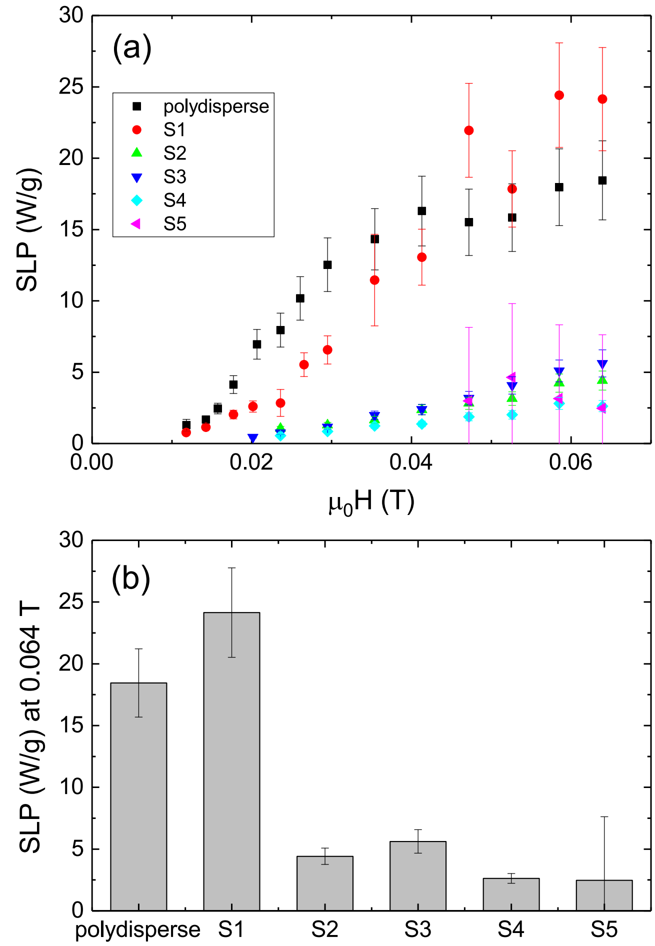

Fig. 4. (a) SLP for the size-separated samples calculated from the slope dT/dt in the temperature range 21.1–21.9 °C at a range of AMF amplitudes. SLP for a polydisperse sample from [10]. (b) SLP at an AMF amplitude of 0.064 T.

The SLP, as calculated from the area enclosed in the dynamic hysteresis loops, is shown in Fig. 6(a) as a function of temperature. This shows that the SLP decreases significantly as the temperature approaches the transition temperature, as expected. The coercivity from the dynamic hysteresis loops is shown in Fig. 6(b) as a function of temperature. This shows that the coercivity of both samples dispersed in H_2O is higher than that of the polydisperse powder sample, presumably because of decreased interactions with neighboring particles. However, under these conditions (AMF, dispersed in H_2O), the coercivity of the smaller particles (S3) is not enhanced relative to the larger particles (S1), as was suggested by previous quasistatic measurements of powder samples[16]. This explains why the SLP is not higher.

4. Discussion

The size-separated gadolinium silicide micro- and nano-particles in this study show a decreasing magnetic transition temperature T_C and decreasing magnetization with decreasing particle size. While previous quasistatic measurements of powder samples had indicated that the coercivity increased with decreasing particle size[16], which could have led to an increase in the SLP in the smaller particles, the current study showed that this did not occur under conditions of hyperthermia (e.g. when the particles were dispersed in H_2O and measured under an AMF). Thus, the smaller particles had a lower SLP, driven solely by their lower magnetization.

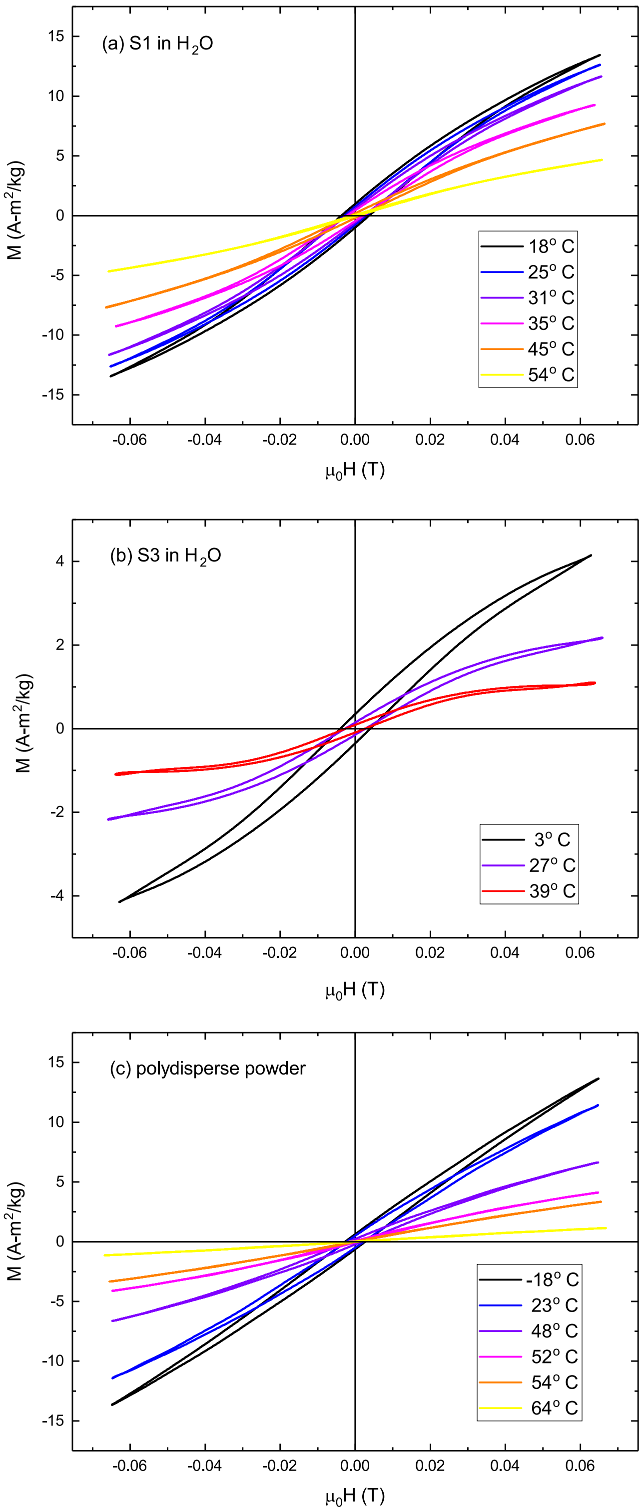

Fig. 5. Dynamic hysteresis loops for several temperatures for (a) sample S1 and (b) sample S3 dispersed in H_2O, and (c) polydisperse powder, measured at a frequency of 224 kHz.

This may be surprising, as coercivity is expected to increase with decreasing particle size in the particle size regime studied here[17,18]. One possible explanation for this is that the T_C of the smaller particles is 10 °C lower than that of the larger particles so that when coercivity is compared for two samples at the same temperature, the smaller particles are nearer their transition than the larger particles and it is not an equal comparison. Another consideration is that, near T_C, there may be considerable fluctuations in the magnetism. Dynamic hysteresis loops measured over a range of frequencies would be a way to explore the effects of fluctuations in these materials near T_C.

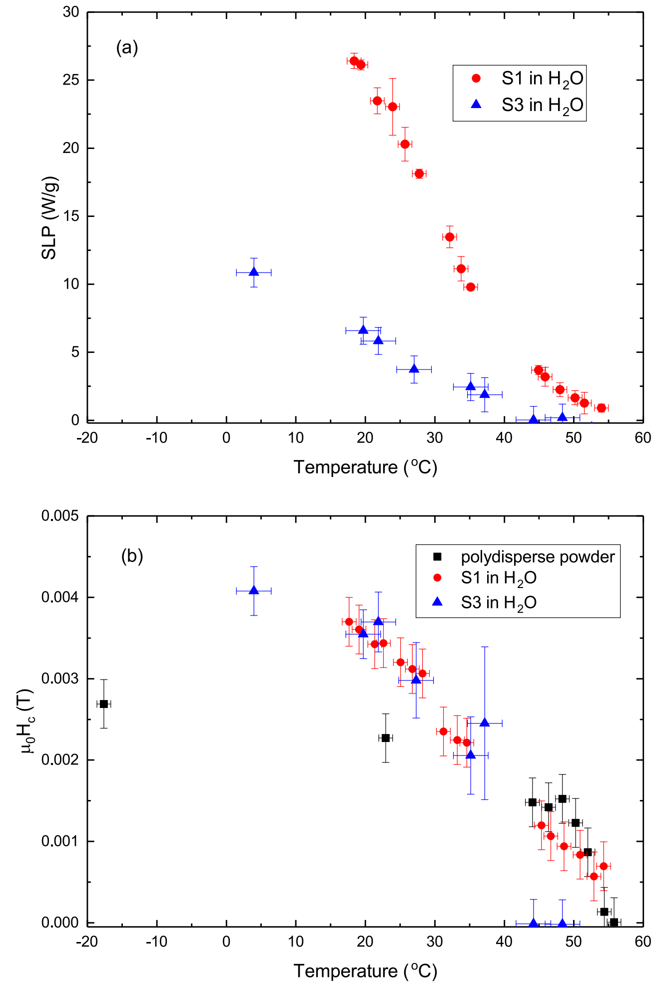

Fig. 6. (a) SLP variation with temperature as calculated from the enclosed area of the dynamic hysteresis loops for samples S1 and S3 dispersed in H_2O. (b) Coercivity $\mu_0 H_c$ from the dynamic hysteresis loops for samples S1 and S3 dispersed in H_2O, and for a polydisperse powder sample.

The results presented here provide some suggestions for improving the T_C and SLP. Of note, the particles dispersed in H_2O had higher coercivity overall than the powder sample, suggesting that a decrease in interparticle interactions was beneficial to the SLP, opening up one avenue for possible improvement. Also, if the decrease in magnetization in the smaller particles is due to the presence of Gd_5Si_3, removal of this impurity phase could increase the magnetization and improve the SLP. Finally, because defects and microstrains introduced by ball-milling are theorized to be responsible for the decrease in T_C, the synthesis methods could be interrogated further to optimize the combination of T_C and SLP.

The SLP values found here, while they can be used to obtain significant heating, are not competitive with iron oxide nanoparticles used for hyperthermia, which can have SLP values of hundreds of W/g[1,23]. These results highlight a challenge for the implementation of self-regulating hyperthermia based on a magnetic transition of any material near the desired operating temperature. In general, H_c and M will decrease as the material approaches T_C; only a very abrupt transition would allow the material to maintain high SLP within a few degrees of T_C. While the "top-down" technique of ball-milling leads to a broader magnetic transition than in the bulk material, even bulk materials have a significantly decreased magnetization and coercivity within a few degrees of T_C[24], the proposed operating range of self-regulating magnetic hyperthermia. Further work on self-regulating hyperthermia should focus on materials with the sharpest transitions.

Self-regulation of hyperthermia by T_C is unlikely to replace other strategies for temperature regulation in situations for which those other strategies are effective[6,7]. However, it could be a valuable tool in situations that are difficult to manage by other means: for example, when tumors have unusual shapes or limited injection sites, or concerns of overheating are particularly worrisome due to nearby sensitive tissues. Given the challenges described here, materials with high magnetization such as rare earth compounds could be the best option to obtain significant heating power near the magnetic transition temperature.

5. Conclusion

Self-regulating magnetic hyperthermia could be a valuable component of magnetic hyperthermia treatment, as it can ensure uniform heating across tumor tissue and margins without requiring a precise distribution of magnetic particles within the tumor and complex modeling of the heating. However, a challenge for the development of self-regulating hyperthermia is the tendency for materials to have low coercivity as they approach the magnetic transition temperature, which limits the specific loss power. Under such conditions, materials with high magnetization, such as rare earth compounds, could be the best option to obtain significant heating. Gadolinium silicide is a promising material because of the tunability of the magnetic transition temperature by either preparation conditions or alloying. In this work, we studied the magnetic properties of ball-milled gadolinium silicide samples with different particle sizes. We found that the magnetization, the Curie temperature, and the specific loss power all decreased as particle size decreased, likely due to defects or microstrains introduced during the ball-milling process, while the coercivity did not differ significantly between particles of different sizes. Future work should explore synthesis techniques to create sub-100 nm particles with T_C near 318 K (45 °C) and with optimized magnetization and specific loss power. The dynamic hysteresis loops of these particles under a range of frequencies should be explored near the transition, as the effects of fluctuations are likely to be frequency-sensitive, and the optimal conditions for the application of self-regulating hyperthermia may differ from those for traditional magnetic hyperthermia.

CRediT authorship contribution statement

Z. Boekelheide: Conceptualization, Methodology, Formal analysis, Investigation, Writing - original draft, Writing - review & editing, Supervision. **S. Hunagund:** Investigation, Writing - original draft. **Z.A. Hussein:** Formal analysis, Investigation. **Jackson T. Miller:** Methodology. **A.A. El-Gendy:** Conceptualization, Supervision, Project administration. **R.L. Hadimani:** Conceptualization, Supervision, Project administration, Funding acquisition.

Declaration of Competing Interest

The authors declare that they have no known competing financial interests or personal relationships that could have appeared to influence the work reported in this paper.

Acknowledgments

Z. A. H. thanks the Bolton Fund for Research Experiences in Math, Biology, Physics, and Chemistry at Lafayette College for support. Thanks to Michael Karner at Lafayette College for making the solenoidal coil and Sena Yevenyo for building the data collection software. Thanks to Shalabh Gupta and Vitalij K. Pecharsky, Ames Laboratory, U.S. Department of Energy, Office of Basic Energy Sciences, Division of Materials Science and Engineering through Iowa State University under Contract DE-AC02-07CH11358, for their assistance in preparing the nanoparticles. Thanks to the Nanomaterials Core Characterization Facility at Virginia Commonwealth University, for XRD, SEM, and VSM use. Work at VCU was partially funded by NSF awards 1610967 and 1726617.

References

[1] E.A. Perigo, G. Hemery, O. Sandre, D. Ortega, E. Garaio, F. Plazaola, F.J. Teran, Fundamentals and advances in magnetic hyperthermia, Appl. Phys. Rev. 2 (2015), 041302.
[2] A. Hervault, N.T.K. Thanh, Magnetic nanoparticle-based therapeutic agents for thermo-chemotherapy treatment of cancer, Nanoscale 6 (2014) 11553.
[3] A.H. El-Sayed, A.A. Aly, N.I. El-Sayed, M.M. Mekawy, A.A. El-Gendy, Calculation of heating power generated from ferromagnetic thermal seed (PdCo-PdNi-CuNi) alloys used as interstitial hyperthermia implants, J. Mater. Sci.: Mater. Med. 18 (2007) 523.
[4] J.L.R. Roti, Cellular responses to hyperthermia (40–46 °C): Cell killing and molecular events, Int. J. Hypertherm. 24 (2008) 3.
[5] J. Overgaard, D.G. Gonzalez, M.C.C.H. Hulshof, G. Arcangeli, O. Dahl, O. Mella, S. M. Bentzen, Hyperthermia as an adjuvant to radiation therapy of recurrent or metastatic malignant melanoma. A multicentre randomized trial by the European Society for Hyperthermic Oncology, Int. J. Hyperthermia 12 (1996) 3.
[6] I. Astefanoaei, A. Stancu, Advanced thermo-mechanical analysis in the magnetic hyperthermia, J. Appl. Phys. 122 (2017), 164701.
[7] M. Salloum, R. Ma, L. Zhu, Enhancement in treatment planning for magnetic nanoparticle hyperthermia: Optimization of the heat absorption pattern, Int. J. Hyperth. 25 (2009) 309.
[8] K.S. Martirosyan, Thermosensitive magnetic nanoparticles for self-controlled hyperthermia cancer treatment, J. Nanomed. Nanotechnol. 3 (2012) 1000e112.
[9] S.N. Ahmad, S.A. Shaheen, Optimization of Gd_5Si_4 based materials: A step toward self-controlled hyperthermia applications, J. Appl. Phys. 106 (2009), 064701.
[10] Z. Boekelheide, Z.A. Hussein, S.M. Harstad, A.A. El-Gendy, R.L. Hadimani, Gd_5Si_4 micro- and nano-particles for self-regulated magnetic hyperthermia, IEEE Trans. Mag. 53 (2017) 5400204.
[11] M.H. Alnasir, M.S. Awan, S. Manzoor, Magnetic and magnetothermal studies of pure and doped gadolinium silicide nanoparticles for self-controlled hyperthermia applications, J. Mag. Magn. Mater. 449 (2018) 137.
[12] F. Holtzberg, R. Gambino, T. McGuire, New ferromagnetic 5:4 compounds in the rare earth silicon and germanium systems, J. Phys. Chem. Solids 28 (11) (1967) 2283.
[13] R.L. Hadimani, S. Gupta, S.M. Harstad, V.K. Pecharsky, D.C. Jiles, Investigation of room temperature ferromagnetic nanoparticles of Gd_5Si_4, IEEE Trans. Mag. 51 (2015) 2504104.
[14] A.A. El-Gendy, S.M. Harstad, V. Vijayaragavan, S. Gupta, V.K. Pecharsky, J. Zweit, R.L. Hadimani, Ferromagnetic Gd5Si4 nanoparticles as T2 contrast agents for MRI, IEEE Magn. Lett. 8 (2017), 1507504.
[15] S.M. Harstad, N. D'Souza, N. Soin, A.A. El-Gendy, S. Gupta, V.K. Pecharsky, T. Shah, E. Siores, R.L. Hadimani, Enhancement of beta phase in PVDF films embedded with ferromagnetic Gd5Si4 nanoparticles for piezoelectric energy harvesting, AIP Adv. 7 (2017), 056411.
[16] S.G. Hunagund, S.M. Harstad, A.A. El-Gendy, S. Gupta, V.K. Pecharsky, R. L. Hadimani, Investigating phase transition temperatures of size separated gadolinium silicide magnetic nanoparticles, AIP Adv. 8 (2018), 056428.
[17] B.D. Cullity, C.D. Graham, Introduction to Magnetic Materials, 2nd Edition, IEEE Press, 2009.
[18] J. Carrey, B. Mehdaoui, M. Respaud, Simple models for dynamic hysteresis loop calculations of magnetic single-domain nanoparticles: Application to magnetic hyperthermia optimization, J. Appl. Phys. 109 (2011), 083921.
[19] V.P. Torchilin, Targeted pharmaceutical nanocarriers for cancer therapy and imaging, AAPS J. 9 (2007) E128.
[20] F. Yuan, M. Dellian, D. Fukumura, M. Leunig, D.A. Berk, V.P. Torchilin, R.K. Jain, Vascular permeability in a human tumor xenograft: Molecular size dependence and cutoff size, Cancer Res. 55 (1995) 3752.
[21] R.R. Wildeboer, P. Southern, Q.A. Pankhurst, On the reliable measurement of specific absorption rates and intrinsic loss parameters in magnetic hyperthermia materials, J. Phys. D: Appl. Phys. 47 (2014), 495003.
[22] E. Garaio, O. Sandre, J.-M. Collantes, J.A. Garcia, S. Mornet, F. Plazaola, Specific absorption rate dependence on temperature in magnetic field hyperthermia measured by dynamic hysteresis losses (ac magnetometry), Nanotechnology 26 (2015), 015704.
[23] Z. Nemati, J. Alonso, I. Rodrigo, R. Das, E. Garaio, J.A. Garcia, I. Orue, M.-H. Phan, H. Srikanth, Improving the Heating Efficiency of Iron Oxide Nanoparticles by Tuning Their Shape and Size, J. Phys. Chem. C 122 (2018) 2367.
[24] J.H. Belo, A.M. Pereira, C. Magen, L. Morellon, M.R. Ibarra, P.A. Algarabel, J. P. Araujo, Critical magnetic behavior of magnetocaloric materials with the Gd_5Si_4-type structure, J. Appl. Phys. 113 (2013), 133909.